Journal of Chromatography A 1715 (2024) 464611

Contents lists available at ScienceDirect

Journal of Chromatography A

journal homepage: www.elsevier.com/locate/chroma

Versatile capillary electrophoresis method for the direct chiral separation of aliphatic and aromatic α-hydroxy acids, β-hydroxy acids and polyhydroxy acids using vancomycin as chiral selector

Julian Urdiain-Arraiza, Benoît Desguin *

Louvain Institute of Biomolecular Science and Technology (LIBST), UCLouvain, 1348, Louvain-La-Neuve, Belgium

ARTICLE INFO

Keywords:
Capillary electrophoresis
Enantiomer separation
Hydroxy acids
Enantioselective analysis
Chiral analysis
Vancomycin

ABSTRACT

Hydroxy acids (HAs) are ubiquitous in nature and play significant roles in various industrial and biological processes. Most HAs harbor at least one chiral center, therefore the development of efficient chiral analysis techniques for HA stereoisomers is of crucial importance across a wide range of fields. A capillary electrophoresis (CE) method was developed for the chiral analysis and quantification of aliphatic and aromatic α-hydroxy acid (AHA) enantiomers, aliphatic β-hydroxy acid (BHA) enantiomers and aliphatic polyhydroxy acid (PHA) stereoisomers. Using a modified partial filling-counter current method with indirect UV detection, high resolution (Rs) was achieved with vancomycin as a chiral selector added to the background electrolyte composed of 10 mM of benzoic acid/L-histidine at pH 5 using a polyacrylamide-coated capillary. This method could be readily applied to the determination of the enantiomers of 12 aliphatic AHAs, 4 aromatic AHAs, 3 aliphatic BHAs, as well as to the determination of the stereoisomers of tartaric acid, 2,3-dihydroxybutanoic acid, 2,3,4,5-tetrahydroxypentanoic acid, and 2,3,4,5,6-pentahydroxyhexanoic acid without the need for sample derivatization. Finally, our study provides a robust and versatile strategy for the chiral and stereoselective analysis of a broad range of hydroxy acid compounds.

1. Introduction

Hydroxy acids (HAs), which are carboxylic acids containing at least one hydroxyl group, are widespread chiral compounds in nature and serve as essential biological building blocks [1]. Among HAs, α-hydroxy acids (AHAs) have their hydroxyl group attached to the second carbon, β-hydroxy acids (BHAs) have their hydroxyl group attached to the third carbon, and polyhydroxy acids (PHAs) possess multiple hydroxyl groups in their structure [2]. In addition to being key metabolites of most metabolic pathways, these acids have considerable market potential and find extensive applications as cosmetics [3,4], drug precursors [5], food components and additives [6–7], building blocks in chemical synthesis [5], monomers for diverse biopolymers [8], and in the production of various basic chemicals [9].

Over the last decades, the chiral analysis of HAs stereoisomers, which include enantiomers and diastereomers, has become of major interest. Different stereoisomers exhibit distinct chemical and biochemical properties, emphasizing the need to of accurately determine and utilize the appropriate stereoisomer for specific applications. Consequently, efficient chiral analysis methods of HA stereoisomers play a crucial role in a wide range of fields. (i) In pharmacology and cosmetics: HAs have significant clinical and pharmacological activity on the skin [2,3]. However, the stereochemistry of compounds is crucial for their therapeutic efficacy and safety [10]. Enantiomeric analysis is essential to ensure the production of stereochemically pure chiral compounds, particularly in pharmaceutical drug research, production, and monitoring processes. (ii) In microbiology: Some HAs are produced by microorganisms and are involved in biodegradation processes. In some cases, the degradation or synthesis rate of a compound may depend on its stereochemistry [11]. Analysis of enantiomers can help researchers investigate the degradation pathways involved. (iii) In food industry: HAs can be important components of food and flavor additives [6,7]. Quality control based on enantioselective analysis of specific enantiomers of HAs can help improve the quality and safety of food products by ensuring that only the desired enantiomer is present. (iv) In industrial chemistry: HA diastereomers may have different physical or chemical properties that affect their performance in industrial processes. Analysis of diastereomers can help optimize industrial production and improve

* Corresponding author.
E-mail address: benoit.desguin@uclouvain.be (B. Desguin).

https://doi.org/10.1016/j.chroma.2023.464611
Received 6 October 2023; Received in revised form 19 December 2023; Accepted 26 December 2023
Available online 27 December 2023

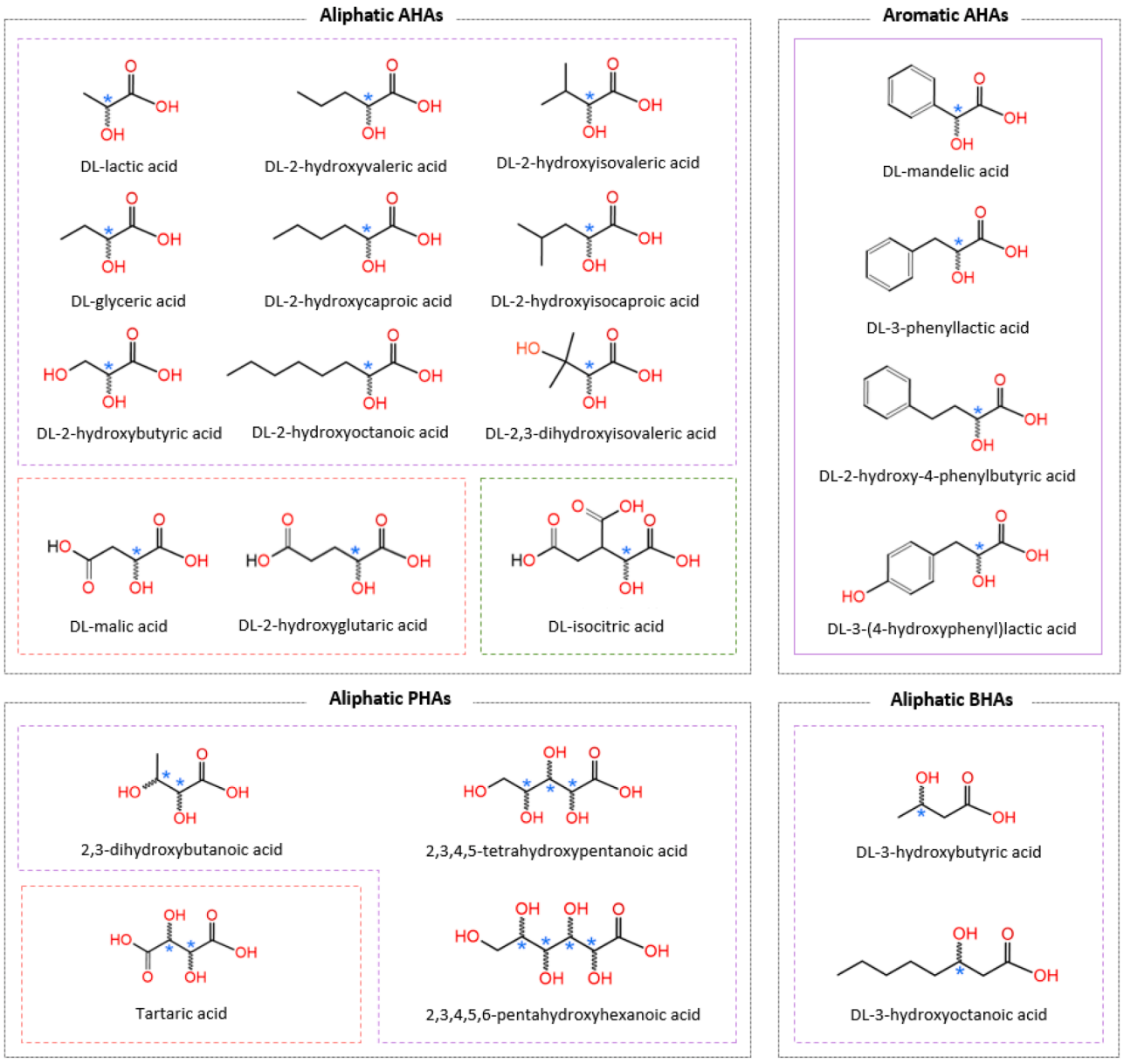

Fig. 1. Chemical structures of the HAs investigated. Monocarboxylic acids are boxed in violet, dicarboxylic are boxed in salmon pink, tricarboxylic acids are boxed in green. Non-UV-absorbing compounds are boxed by a dashed line, while UV-absorbing compounds are boxed by a solid line. The chiral carbons are indicated by blue asterisk and are left achiral for simplification.

the yield and quality of the final product. (v) In clinical analysis: Alterations in the expected levels of many AHAs have been associated to specific diseases or health benefits [12]. Their enantioselective analysis is consequently a major concern in biomarker studies and clinical analysis [13–14]. Overall, the chiral analysis of hydroxy acid stereoisomers is important to ensure the safety, efficacy, and environmental impact of drugs, food additives, and industrial products.

Direct chiral analysis of HAs involves the formation of transient diastereomeric complexes and does not require derivatization. In contrast, indirect chiral analysis of HAs involves the formation of stable diastereomers and requires derivatization [15]. A variety of different analytical methods have been employed to separate underivatized HAs. Aliphatic AHA enantiomers have been separated by CE [16,17], HPLC [13,18,19], HPLC-MS [20], LC-MS/MS [21], and ligand exchange CE (LE-CE) [22]. The separation of aromatic AHA enantiomers has been accomplished using techniques such as CE [23,24], LE-CE [25], ligand-exchange capillary electrochromatography (LE-CEC) [26], ligand exchange high-speed countercurrent chromatography (LE-HSCCC) [27], and HPLC [28,29]. Similarly, aliphatic BHA enantiomers have been separated by HPLC [13,30], HPLC-ESI-MS/MS [31], and UHPLC-MS/MS [32]. To date, no CE method has been described for the chiral analysis of underivatized BHAs or PHAs, except for DL-tartaric acid using CE [33–34] or HPLC [13], to the best of our knowledge.

Among these methods, CE has proven to be a cheap, simple and highly effective technique for the analysis of enantiomers without the need for derivatization or polar solvents, and it offers versatile capabilities due to the availability of numerous chiral selectors [35,36]. In particular, CE excels in the analysis of charged solutes and constitutes a powerful tool for the analysis of carboxylic acids in general [37]. Moreover, of all the analytical methods available, none yet offers a general procedure for the chiral analysis of different types of HAs. The lack of a chiral analysis method for PHAs and of a versatile procedure for chiral analysis of different types of HAs leaves a major gap in the field of chiral analysis of these valuable compounds.

This study addresses this gap in the field of chiral analysis of HA stereoisomers. We have developed a versatile and highly efficient CE method that allows the direct chiral analysis and quantification of a broad spectrum of HA stereoisomers, including aliphatic and aromatic AHAs enantiomers, aliphatic BHAs enantiomers, and aliphatic PHAs stereoisomers.

The chemical structures of the chiral hydroxy acids investigated are shown in Fig. 1.

2. Material and methods

2.1. Chemicals and reagents

All chemicals were either of analytical grade or reagent grade. D-lactic acid (sodium salt), L-lactic acid (sodium salt), D-glyceric acid (sodium salt), L-glyceric acid (sodium salt), D-malic acid, L-malic acid, D-2-hydroxybutyric acid, L-2-hydroxybutyric acid, DL-2-hydroxycaproic acid, DL-2-hydroxyisocaproic acid, L-2-hydroxyisocaproic acid, D-2-hydroxyisovaleric acid, L-2-hydroxyisovaleric acid, DL-2-hydroxyoctanoic acid, D-2,3-dihydroxyisovaleric acid (sodium salt), L-2,3-dihydroxyisovaleric acid (sodium salt), D-2-hydroxyglutaric acid (disodium salt), L-2-hydroxyglutaric acid (disodium salt), D-3-phenyllactic acid, L-3-phenyllactic acid, D-2-hydroxy-4-phenylbutyric acid, DL-mandelic acid, D-mandelic acid, D-ribonic acid (lithium salt), L-ribonic acid (lithium salt), D-arabinonic acid (sodium salt), D-lyxonic acid (potassium salt), L-lyxonic acid (potassium salt), D-gluconic acid (sodium salt), D-altronic acid (lithium salt), L-gulonic acid (lactone), D-gulonic acid (lithium salt), benzoic acid and L-histidine were purchased from Sigma-Aldrich. L-2-hydroxyvaleric acid, L-2-hydroxycaproic acid, L-2-hydroxy-4-phenylbutyric acid, DL-3-hydroxyoctanoic acid, L-arabinonic acid (lithium salt), D-xylonic acid (lithium salt), L-xylonic acid (lithium salt), L-gluconic acid (lactone), D-galactonic acid (lactone), L-galactonic acid (lactone), D-allonic acid (lactone), L-allonic acid (lactone), D-mannonic acid (lactone), L-mannonic acid (lactone), D-idonic acid (lactone), L-idonic acid (lactone), D-talonic acid (lactone) were purchased from Biosynth. L-talonic acid (potassium salt) was purchased from Omicro Biochemicals Inc. L-altronic acid was produced in our lab by the C2-epimerization of L-allonic acid (data not published). DL-2-hydroxyvaleric acid was purchased from Acros Organics. D-2-hydroxyoctanoic acid was purchased from BLDpharm. 4-Deoxy-D-erythronic acid (sodium salt hydrate), 4-Deoxy-L-erythronic acid (sodium salt hydrate), 4-Deoxy-D-threonic acid (sodium salt hydrate), 4-Deoxy-L-threonic acid (sodium salt hydrate), DL-3-hydroxybutyric acid, L-3-hydroxybutyric acid were purchased from Supelco. Vancomycin was purchased from Thermo Fisher Scientific.

2.2. Apparatus and separation procedure

All electrophoretic runs were performed on the CE system Capel 105 M from Lumex Instrument in a polyacrylamide-coated capillary with 50 μm i.d. x 122/112.5 cm total/effective length. Prior to the first experiment of the day, the coated capillary was rinsed for 10 min with the BGE consisting of 10 mM benzoic acid/L-histidine at pH 5.0. To control the partial filling process and to prevent the presence of vancomycin in the detector window, the BGE supplemented with vancomycin was introduced into the capillary at a pressure of 1000 mbar for 145 s. The positioning of vancomycin just before the detection window was fine-tuned based on absorbance measurements during capillary filling. Samples were injected at a pressure of 30 mbar for 5 s. A counter current method was employed throughout the analysis with an applied voltage of −25 kV. Detection was performed in the indirect UV photometric detection mode at 230 nm. The capillary temperature was maintained at 20 °C during all steps. Between runs, the capillary was rinsed with BGE at 1000 mbar for 5 min. At the end of the day, the capillary was rinsed with distilled water for 10 min and both ends of the capillary were kept in water.

2.3. Capillary-coating procedure

The coating process of the capillary inner surface by polyacryamide was based on previously published procedures [38,39]. The fused-silica capillary was rinsed with 0.5 M HCl for 30 min and then with deionized water for 30 min. After rinsing, the capillary was silylated by flushing with a 3 % v/v solution of 3-(trimethoxysilyl)propylmethacrylate in 50 % aqueous acetone for 1 h. After the silylation process, the capillary was rinsed with deionized water for 25 min. The final polymerization step was performed by flushing of 3% w/v solution of acrylamide in deionized water with additions of 0.05% w/v ammonium persulfate and 0.04 % v/V tetramethylethylenediamine for 45 min for the capillary with 50 μm i.d. x 122/112 cm total/effective length and 1 h for the capillary with 50 μm i.d. x 54/46 cm total/effective length. After the coating procedure, the capillary was rinsed with deionized water at 2000 mbar for 2 h.

2.4. Effective electrophoretic mobility calculation

The effective electrophoretic mobilities were calculated using Eq. (1), with water as neutral marker to determine the electroosmotic flow (EOF) [40]:

$$\mu_{eff} = \mu_{app} - \mu_{EOF} = \frac{L_e \cdot L_t}{U} \cdot \left(\frac{1}{t_m} - \frac{1}{t_{EOF}}\right) \quad (1)$$

where μ_{eff} is the effective electrophoretic mobility of the analyte (m^2 V^{-1} s^{-1}), μ_{app} is the apparent electrophoretic mobility of the analyte (m^2 V^{-1} s^{-1}), μ_{EOF} is the electroosmotic mobility (m^2 V^{-1} s^{-1}), t_m is the migration time of the analyte (s), t_{EOF} is the migration time of the neutral marker (s), L_t is the total length of the capillary (m), L_e is the effective length of the capillary (m), and U is the applied voltage (V).

2.4. Complex matrices preparation

GntE1-catalyzed epimerization reactions of D-gluconate to D-mannonate were made in a 200 μl final volume containing 10 mM of D-gluconate, 5 μM of in vitro synthesized NPN, 1 μM of purified GntE1 and 0.1 M Tris-HCL buffer, pH 8, incubated for 0, 1, 2 or 3 h. IDH-catalyzed dehydrogenation reactions of D-isocitrate to 2-ketoglutarate and CO_2 were made using the D-isocitric Acid Assay Kit from Megazyme in a 200 μl final volume containing 2 mM of D-isocitrate, 5 mM of $NADP^+$, 50 nM of IDH and the kit buffer, pH 7.8, incubated for 0, 5, 10 or 15 min. Reactions were stopped by heat inactivation at 90 °C for 10 min.

A 530 mg zinc-gluconate dietary supplement tablet (Now Foods) contained 50 mg of Zinc, 353 mf of D-gluconate, microcrystalline cellulose, vegetarian coating, magnesium stearate and silicon dioxide. Matrices of 0.5 mg/ml zinc-gluconate dietary supplement were prepared by grinding tablets and resolubilizing them in boiling water ($n = 3$).

3. Results and discussion

3.1. Method development and robustness

For our method, we used a background electrolyte (BGE) consisting of an aqueous buffer of 10 mM benzoic acid/L-histidine at pH 5. Vancomycin was chosen as a chiral selector because it is a macrocyclic glycopeptide antibiotic (MA) commonly used in capillary electrophoresis for the enantioseparation of chiral compounds with carboxylic groups [41–43].

We opted for a hydrodynamic partial-filling countercurrent separation method with indirect UV detection in a polyacrylamide-coated capillary, as this method provides several advantages. First, indirect UV detection enables the analysis of non-UV-absorbing compounds such as aliphatic HAs, thus broadening the range of detectable analytes.

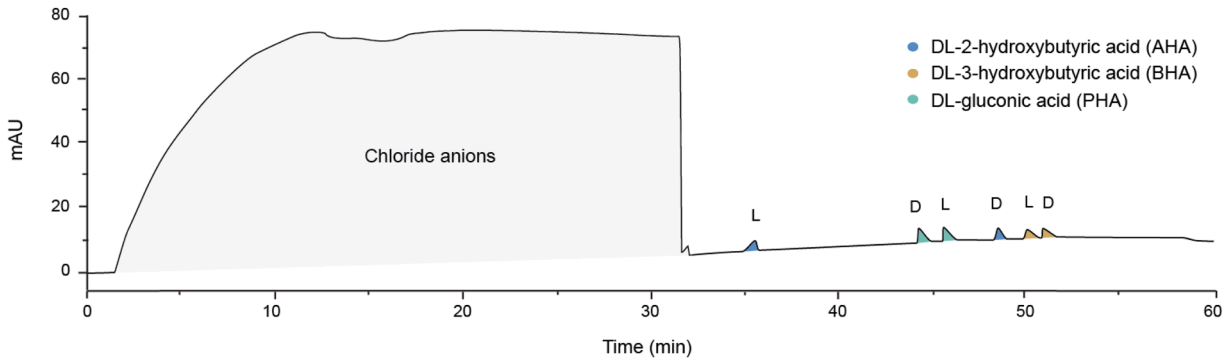

Fig. 2. EPG of the simultaneous enantioseparation of the enantiomers of an AHA, a BHA and a PHA. All enantiomers are at a concentration of 8 mM. Electrophoretic conditions: polyacrylamide-coated capillary, 122 (112) cm x 50 μm; BGE, 10 mM benzoic acid/L-histidine, pH 5, and 25 mM vancomycin; partial filling, 145 s at 1000 mbar; injection, 5 s at 30 mbar; voltage, –25 kV; temperature, 20 °C; indirect detection at 230 nm.

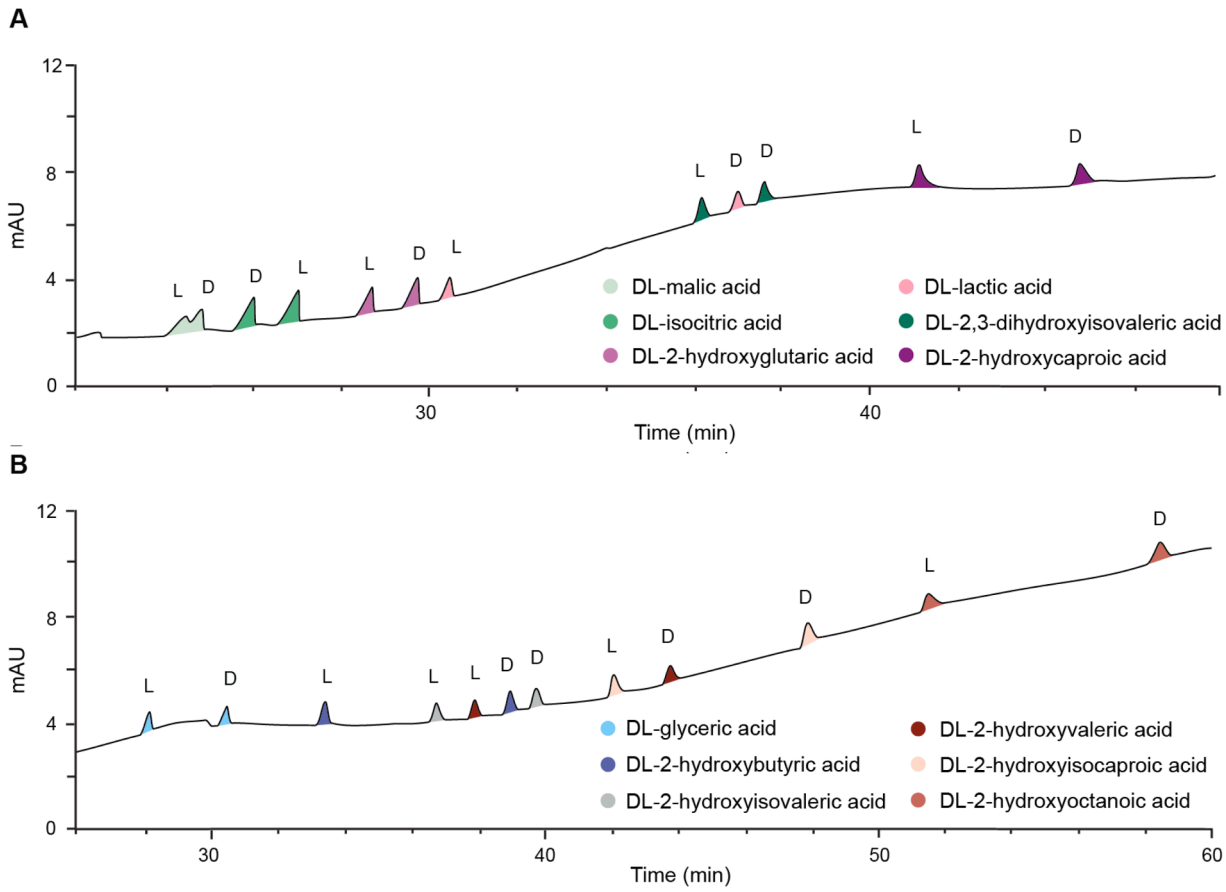

Fig. 3. Simultaneous enantioseparation of aliphatic AHA enantiomers. All enantiomers are at a concentration of 1 mM. (A) Vancomycin concentration 10 mM, other electrophoretic conditions as in Fig. 2. (B) Vancomycin concentration 15 mM, other electrophoretic conditions as in Fig. 2.

Second, the polyacrylamide coating reduces the adsorption of analytes and chiral selectors on the capillary wall, resulting in improved separation efficiency and reduced EOF [44]. Third, the partial filling technique allows for improved analyte detectability by eliminating vancomycin from the detection cell, thereby minimizing its interference. This is particularly important since vancomycin absorbs strongly in the UV region [45,46]. Lastly, the countercurrent separation method enhances the separation of enantiomers due to the opposite migration directions of the HAs and the vancomycin cations [44,47].

Fig. 2 shows an electropherogram (EPG) obtained with our method displaying the simultaneous enantioseparation of the enantiomers of an AHA (DL-2-hydroxybutyric acid), a BHA (DL-3-hydroxybutyric acid), and a PHA (DL-gluconic acid). A large absorbing zone was observed at the beginning of each run. This was previously shown by Bednar P. et al. that it is due to the presence of chloride anions associated with the vancomycin cations [48]. By using a partial-filling countercurrent separation method, the vancomycin cations migrate away from the detection window, while the chloride anions and hydroxy acid anions migrate towards the detection window. The chloride anions are detected first due to their higher mobility within the system. The area of the peak corresponding to chloride anions is directly proportional to both the concentration of vancomycin and the effective length of the capillary used for chiral separation. In general, when using 25 mM vancomycin, the chloride anion peak ends at 31 min using a capillary with an effective

Table 1
Separation data of AHA and BHA enantiomers. All separations were performed with 0.5 mM of each enantiomer. Rs = resolution; α = separation factor; MW = molecular weight (g/mol); MO = migration order. Vancomycin concentrations as indicated, other electrophoretic conditions as in Fig. 2..

	DL-enantiomers	MW	Vancomycin	MO	α	Rs
Aliphatic AHAs	DL-isocitric acid	192.1	12	$D < L$	1.06	4.3
	DL-malic acid	134.1		$L < D$	1.03	1.5
	DL-lactic acid	90.1	15		1.43	28.3
	DL-glyceric acid	106.1			1.11	6.3
	DL-2-hydroxyglutaric acid	148.1			1.07	4.8
	DL-2-hydroxybutyric acid	104.1	25		1.29	20.4
	DL-2-hydroxyvaleric acid	118.1			1.32	26.1
	DL-2-hydroxyisovaleric acid	118.1			1.16	11.3
	DL-2-hydroxycaproic acid	132.2			1.26	21.8
	DL-2-hydroxyisocaproic acid	132.2			1.28	23.2
	DL-2,3-dihydroxyisovaleric acid	134.1			1.11	8.3
	DL-2-hydroxyoctanoic acid	160.2			1.22	18.3
Aromatic AHAs	DL-mandelic acid	152.2			1.02	1.7
	DL-3-phenyllactic acid	166.2			1.38	29.4
	DL-3-(4-hydroxyphenyl)lactic acid	182.2			1.47	43.2
	DL-2-hydroxy-4-phenylbutyric acid	180.2			1.16	15.3
Aliphatic BHAs	DL-3-hydroxybutyric acid	104.1			1.02	1.8
	DL-3-hydroxyoctanoic acid	160.2			1.03	2.7

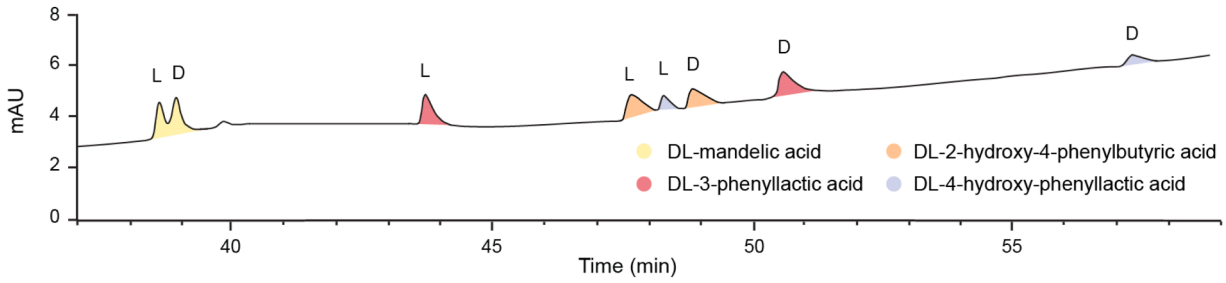

Fig. 4. Simultaneous enantioseparation of aromatic AHA enantiomers. All enantiomers are at a concentration of 2 mM. Vancomycin concentration 10 mM, other electrophoretic conditions as in Fig. 2.

length of 112 cm, and at 8 min using a capillary with an effective length of 46 cm.

For the separation of DL-2-hydroxybutyric acid, DL-3-hydroxybutyric acid and DL-gluconic acid, we calculated the intra-day and inter-day relative standard deviation (R.S.D.) for various parameters. Inter-day R.S.D. values are between 0.5 % and 3.9 % for peak areas, 0.1 % and 1.1 % for migration times, 2.8 % and 4.9 % for resolutions and 0.2 % and 0.7 % for separation factors. Intra-day R.S.D. values are between 1.1 % and 4.9 % for peak areas, 1.8 % and 3.5 % for migration times, 3.5 % and 6.9 % for resolutions and 0.3 % and 1.3 % for separation factors. These low inter- and intra-day variabilities demonstrate the robustness of our method for the chiral separation of AHAs, BHAs and PHAs (Table S1).

3.2. Chiral separation of AHA enantiomers

3.2.1. Chiral separation of aliphatic AHA enantiomers

Our method allowed the highly efficient chiral analysis of 12 different aliphatic AHAs which are non-UV-absorbing: DL-lactic acid, DL-glyceric acid, DL-2-hydroxybutyric acid, DL-2-hydroxycaproic acid, DL-2-hydroxyisocaproic acid, DL-malic acid, DL-2-hydroxyvaleric acid, DL-2-hydroxyisovaleric acid, DL-2-hydroxyoctanoic acid, DL-2,3-dihydroxyisovaleric acid, DL-2-hydroxyglutaric acid, and DL-isocitric acid (Fig. 3A and B). Baseline resolution (Rs $\geq$ 1.5) was obtained for all aliphatic AHA enantiomers (Table 1). This demonstrates that our protocol allows the chiral separation of monocarboxylic (e.g. lactic acid), dicarboxylic (e.g. 2-hydroxyglutaric acid) and tricarboxylic (e.g. isocitric acid) AHA enantiomers.

The migration times of the AHA anions positively correlate with their molecular weight and negatively correlate with the number of negative charges (Table 1 and Fig. 3).

Lactic acid is one of the AHAs whose chiral separation has been most widely reported in the literature, with Rs values ranging from 1.25 to 3.8 [16–18,20,49–52]. In comparison, our method allows the chiral separation of DL-lactic acid with a Rs of 28.3 (Table 1).

3.2.2. Chiral separation of aromatic AHA enantiomers

Aromatic AHAs have wide-ranging applications for the production of biocompatible and biodegradable polymers, as antimicrobial compounds, for biomarker usage, and as versatile chiral building blocks for the large-scale production of active pharmaceutical compounds including antibiotics, antitumor, and antiobesity agents [5,28]. Fig. 4 shows an efficient chiral separation of four different aromatic AHAs which are UV-absorbing due to their aromatic ring acting as a chromophore: DL-mandelic acid, DL-3-phenyllactic acid, DL-3-(4-hydroxyphenyl)lactic acid, and DL-2-hydroxy-4-phenylbutyric acid. Baseline resolution was obtained for all aromatic AHA enantiomers (Table 1).

3.3. Chiral separation of aliphatic BHA enantiomers

Aliphatic BHAs have multifaceted applications, serving as starting materials for chemical synthesis and biochemical transformations for the production of optically active bioactive compounds such as vitamins, antibiotics, antifungals, pheromones and flavors [53,54]. For example, 3-hydroxybutyrate has gained significant interest in medicine, dietetics, and for the biodegradable plastics industry [55]. In addition, many aliphatic BHAs are important chiral building blocks for lipopeptide synthesis and as disease-related biomarkers [56,57]. As such, enantioselective analysis of aliphatic BHAs is crucial for an unbiased biological

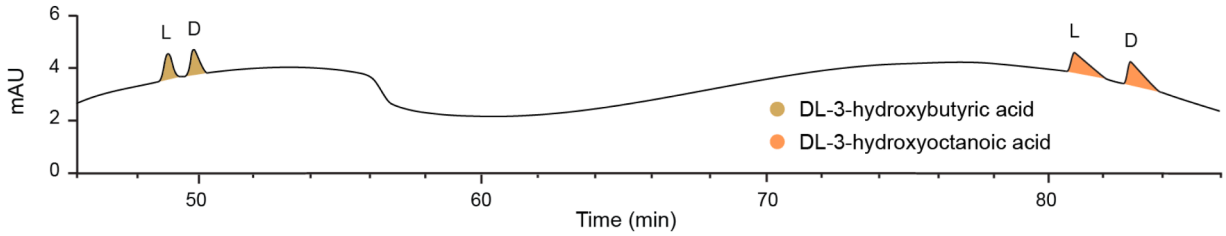

Fig. 5. Simultaneous enantioseparation of BHA enantiomers. All enantiomers are at a concentration of 2 mM. Electrophoretic conditions as in Fig. 2.

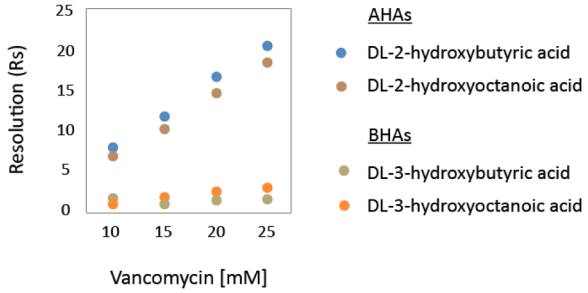

Fig. 6. Chiral separation of AHA enantiomers compared to the chiral separation of BHA enantiomers. Vancomycin concentrations as indicated, other electrophoretic conditions as in Fig. 2.

or clinical interpretation.

However, in spite of the advanced state of enantiomer separation methods, the direct or indirect chiral separation of aliphatic BHAs remains a challenge in comparison to the chiral separation of AHAs. Currently, no CE method has been published for the enantioseparation of BHAs. Using our method, both D- and L- enantiomers of 3-hydroxybutyric acid and of 3-hydroxyoctanoic acid were separated (Fig. 5). Baseline resolution was obtained for all aliphatic BHA enantiomers (Table 1). Enantioselectivity may also be expected for aliphatic BHA with carbon chain lengths between four and eight carbons, as resolution improved with carbon chain length from four to eight.

When comparing the chiral separation of AHA and BHA enantiomers, we observed that the resolution was 8–12 times lower for BHA enantiomers, thus requiring a higher concentration of vancomycin for their efficient separation (Fig. 6). Vancomycin probably interacts less specifically with the molecules when the hydroxyl group is located on C3 rather than on C2, as the distance and flexibility between the carboxyl group and both the hydroxyl and carbon side chain increase.

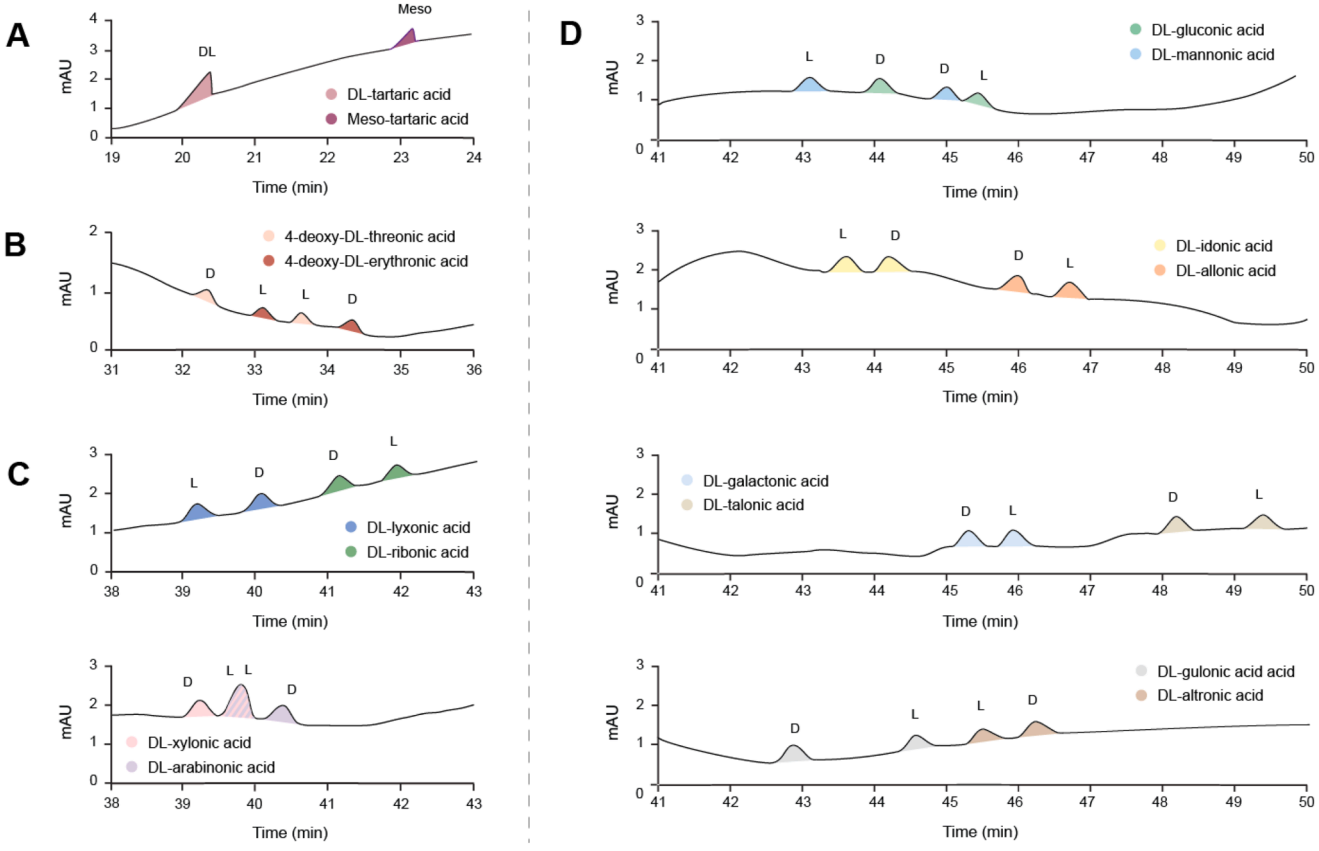

Fig. 7. Chiral separation of PHAs stereoisomers. All enantiomers are at a concentration of 0.5 mM. (A) Chiral separations of tartaric acid stereoisomers. Electrophoretic conditions: vancomycin 5 mM. (B) Chiral separations of 2,3-dihydroxybutanoic acid stereoisomers. Electrophoretic conditions: vancomycin 20 mM. (C) Chiral separations of 2,3,4,5-tetrahydroxypentanoic acid stereoisomers. (D) Chiral separations of 2,3,4,5,6-pentahydroxyhexanoic acid stereoisomers. Other electrophoretic conditions as in Fig. 2 for A, B, C and D.

Table 2
Chiral separation of tartaric acid stereoisomers. Enantiomers (yellow boxes), C-2 and C-3 epimers (red boxes). NS = not separated. The resolution is underlined and the separation factor is italicized. Vancomycin concentration 5 mM, other electrophoretic conditions as in Fig. 2.

	Resolution (Rs) and separation factor (α)			
	D-tartaric acid (2S,3S)		L-tartaric acid (2R,3R)	
L-tartaric acid (2R,3R)	NS			
Meso-tartaric acid (2R,3S) or (2S,3R)	5.7	*1.12*	5.7	*1.12*

Table 3
Chiral separation of 2,3-dihydroxybutanoic acid stereoisomers. Enantiomers (yellow boxes), C-2 epimers (purple boxes), C-3 epimers (blue boxes). D-4DE = 4-deoxy-D-erythronic acid (2R,3R), L-4DE = 4-deoxy-L-erythronic acid (2S,3S), D-4DT = 4-deoxy-D-threonic acid (2S,3R), L-4DT = 4-deoxy-L-threonic acid (2R,3S), NS = not separated. The resolution is underlined and the separation factor is italicized. Vancomycin concentration 20 mM, other electrophoretic conditions as in Fig. 2.

	Resolution (Rs) and separation factor (α)					
	D-4DE (2R,3R)		L-4DE (2S,3S)		D-4DT (2S,3R)	
L-4DE (2S,3S)	2.8	*1.04*				
D-4DT (2S,3R)	4.3	*1.07*	1.9	*1.03*		
L-4DT (2R,3S)	1.5	*1.02*	1.3	*1.02*	3.1	*1.05*

Table 4
Chiral separation of 2,3,4,5-tetrahydroxypentanoic acid stereoisomers. Enantiomers (yellow boxes), C-2 epimers (purple boxes), C-3 epimers (blue boxes), C-4 epimers (gray boxes). D-xylo = D-xylonic acid (2R,3S,4R), L-xylo = L-xylonic acid (2S,3R,4S), D-lyxo = D-lyxonic acid (2S,3S,4R), L-lyxo = L-lyxonic acid (2R,3R,4S), D-ribo = D-ribonic acid (2R,3R,4R), L-ribo = L-ribonic acid (2S,3S,4S), D-ara = D-arabinonic acid (2S,3R,4R), L-ara = L-arabinonic acid (2R,3S,4S), NS = not separated. The resolution is underlined and the separation factor is italicized. Electrophoretic conditions as in Fig. 2.

	Resolution (Rs) and separation factor (α)													
	D-xylo		L-xylo		D-lyxo		L-lyxo		D-ribo		L-ribo		D-ara	
L-xylo	1.1	*1.02*												
D-lyxo	1.6	*1.02*	0.6	*1.01*										
L-lyxo	NS		1.1	*1.02*	1.6	1.02								
D-ribo	3.4	*1.05*	2.2	*1.03*	1.8	*1.03*	3.4	1.05						
L-ribo	4.9	*1.07*	3.5	*1.05*	3.1	*1.04*	4.9	1.07	1.4	1.02				
D-ara	2.4	*1.03*	1.4	*1.02*	1.1	*1.02*	2.4	1.03	1.2	1.02	2.6	1.03		
L-ara	1.1	*1.02*	NS		0.6	*1.01*	1.1	1.02	2.2	1.03	3.5	1.05	1.4	1.02

3.4. Chiral separation of aliphatic PHA stereoisomers

While underivatized AHAs and BHAs have been previously enantioseparated using various chiral methods, analogous applications for underivatized PHAs are absent in the scientific literature, except for tartaric acid. In this study, we analyzed the enantiomers and diastereomers of tartaric acid (DL- and meso-tartaric acid) (Fig. 7A), 2,3-dihydroxybutanoic acid (4-deoxy-DL-erythronic acid and 4-deoxy-DL-threonic acid) (Fig. 7B), 2,3,4,5-tetrahydroxypentanoic acid (DL-ribonic acid, DL-arabinonic acid, DL-xylonic acid, and DL-lyxonic acid) (Fig; 7C) and 2,3,4,5,6-pentahydroxyhexanoic acid (DL-gluconic acid, DL-allonic acid, DL-gulonic acid, DL-altronic acid, DL-talonic acid, DL-galactonic acid, DL-idonic acid, and DL-mannonic acid) (Fig. 7D). All of these compounds are aldonic sugar acids, except tartaric acid which is an aldaric sugar acid. The chiral separation of sugar acids could become of utmost interest since these acids are widely distributed in nature and are used for numerous applications, such as detergent components, pH regulators, corrosion inhibitors, additives in the food industry, monomers for polymeric materials, and biodegradable chelators for pharmaceuticals [58].

Most reports on the chiral separation of tartaric acid only mention the separation of its enantiomers, D- and L-tartaric acid. In our case, the separation of tartaric acid enantiomers was not successful, but we could achieve the separation of its diastereomers, D- from meso- and L- from *meso* (Table 2).

With our method, we were able to differentiate all six possible stereoisomer combinations of 2,3-dihydroxybutanoic acid (Table 3), 24 out of the 28 possible stereoisomer combinations of 2,3,4,5-tetrahydroxypentanoic acid (Table 4), and 101 out of the 120 possible stereoisomer combinations of 2,3,4,5,6-pentahydroxyhexanoic acid (Table 5). When a Rs cut-off of 1.5 is applied, which corresponds to the baseline separation of two different peaks, we were still able to differentiate five out of six possible stereoisomer combinations of 2,3-dihydroxybutanoic acid, 15 out of 28 possible stereoisomer combinations of 2,3,4,5-tetrahydroxypentanoic acid, and 89 out of 120 possible stereoisomer combinations of 2,3,4,5,6-pentahydroxyhexanoic acid (Table 6). This demonstrates that our method is capable of differentiating the vast majority of PHA stereoisomers.

3.5. Migration order and electrophoretic mobilities

When analyzing a mixture of unknown enantiomeric ratio, the knowledge of the migration order allows direct identification of the L- and D-enantiomers. For all AHAs and BHAs, except for isocitric acid, the L-enantiomer with 2S stereochemistry migrated faster than the D-enantiomer with 2R stereochemistry (Figs. 3, 4, 5 and Table 1).

For tartaric acids, L- and D-tartaric acid migrated faster than meso-tartaric acid (Fig. 8A).

For enantiomeric pairs or C2 epimeric pairs of 2,3-dihydroxybutanoic acids, the enantiomer or C2 epimers with a 2S stereochemistry migrated faster than the enantiomer or C2 epimers with a 2R stereochemistry. Conversely, for enantiomeric pairs or C2 epimeric pairs of

Table 5
Chiral separation of 2,3,4,5,6-pentahydroxyhexanoic acid stereoisomers. Enantiomers (yellow boxes), C-2 epimers (purple boxes), C-3 epimers (blue boxes), C-4 epimers (gray boxes), C-5 epimers (green boxes). D-glu = D-gluconic acid (2R,3S,4R,5R), L-glu = L-gluconic acid (2S,3R,4S,5S), D-gal = D-galactonic acid (2R,3S,4S,5R), L-gal = L-galactonic acid (2S,3R,4R,5S), D-aln = D-allonic acid (2R,3R,4R,5R) , L-aln = L-allonic acid (2S,3S,4S,5S), D-ma = D-mannonic acid (2S,3S,4R,5R), L-ma = L-mannonic acid (2R,3R,4S,5S), D-ido = D-idonic acid (2S,3R,4S,5R) , L-ido = L-idonic acid (2R,3S,4R,5S), D-alt = D-altronic acid (2S,3R,4R,5R), L-alt = L-altronic acid (2R,3S,4S,5S), D-tal = D-talonic acid (2S,3S,4S,5R), L-tal = L-talonic acid (2R,3R,4R,5S), D-gul = D-gulonic acid (2R,3R,4S,5R); L-gul = L-gulonic acid (2S,3S,4R,5S); NS = not separated. The resolution is underlined and the separation factor is italicized. Electrophoretic conditions as in Fig. 2.

	Resolution (Rs) and separation factor (α)														
	D-glu	L-glu	D-gal	L-gal	D-aln	L-aln	D-ma	L-ma	D-ido	L-ido	D-alt	L-alt	D-tal	L-tal	D-gul
L-glu	1.8 *1.02*														
D-gal	1.7 *1.02*	0.5 *1.01*													
L-gal	2.8 *1.03*	0.8 *1.01*	1.1 *1.01*												
D-aln	2.8 *1.03*	0.8 *1.01*	1.1 *1.01*	NS											
L-aln	3.9 *1.05*	2.2 *1.02*	2.4 *1.03*	1.2 *1.01*	1.2 *1.01*										
D-ma	1.3 *1.02*	0.7 *1.01*	0.8 *1.01*	1.7 *1.02*	1.7 *1.02*	2.5 *1.03*									
L-ma	2.2 *1.03*	3.8 *1.05*	3.5 *1.04*	4.7 *1.06*	4.7 *1.06*	5.5 *1.07*	2.9 *1.03*								
D-ido	NS	1.8 *1.02*	1.7 *1.01*	2.8 *1.03*	2.8 *1.03*	3.9 *1.05*	1.3 *1.01*	2.2 *1.02*							
L-ido	1.1 *1.01*	2.6 *1.03*	2.4 *1.03*	3.8 *1.05*	3.8 *1.05*	4.8 *1.06*	2 *1.02*	1.2 *1.01*	1.1 *1.01*						
D-alt	3.3 *1.04*	1.6 *1.02*	1.8 *1.02*	0.8 *1.01*	0.8 *1.01*	0.4 *1.01*	2.3 *1.03*	5.4 *1.07*	3.3 *1.04*	4.4 *1.05*					
L-alt	1.8 *1.02*	NS	0.5 *1.01*	0.8 *1.01*	0.8 *1.01*	2.2 *1.02*	0.7 *1.01*	3.8 *1.05*	1.8 *1.02*	2.6 *1.03*	1.6 *1.02*				
D-tal	7.7 *1.1*	5.4 *1.07*	5.7 *1.07*	4.7 *1.06*	4.7 *1.06*	3.6 *1.05*	6.2 *1.08*	9.6 *1.12*	7.7 *1.1*	8.6 *1.11*	4.1 *1.05*	5.4 *1.07*			
L-tal	10.8 *1.13*	8.2 *1.11*	8.4 *1.11*	7.6 *1.1*	7.6 *1.1*	6.4 *1.08*	9.1 *1.11*	12.4 *1.16*	10.8 *1.13*	11.6 *1.14*	6.9 *1.09*	8.2 *1.11*	2.7 *1.03*		
D-gul	2.6 *1.03*	4.7 *1.06*	4.4 *1.05*	5.3 *1.07*	5.3 *1.07*	6.5 *1.08*	3.8 *1.05*	0.8 *1.01*	2.6 *1.03*	1.9 *1.02*	6 *1.08*	4.7 *1.06*	10.4 *1.13*	13.1 *1.17*	
L-gul	0.6 *1.01*	1.3 *1.02*	1.1 *1.01*	2.3 *1.03*	2.3 *1.03*	3.3 *1.04*	0.5 *1.01*	2.4 *1.03*	0.6 *1.01*	1.5 *1.02*	2.8 *1.03*	1.3 *1.02*	6.8 *1.09*	10.1 *1.13*	3.2 *1.04*

Table 6
Efficiency of the chiral separation of PHA stereoisomers. Electrophoretic conditions as in Fig. 7.

Stereoisomers of	MW (g/mol)	# of Rs ≥ 1	# of Rs ≥ 1.5
Tartaric acid	150.1	2/3	2/3
2,3-dihydroxybutanoic acid	120.1	6/6	5/6
2,3,4,5-tetrahydroxypentanoic acid	166.1	24/28	15/28
2,3,4,5,6-pentahydroxyhexanoic acid	196.2	101/120	89/120

2,3,4,5-tetrahydroxypentanoic acids and 2,3,4,5,6-pentahydroxyhexanoic acids, the enantiomer or C2 epimers with a 2R stereochemistry migrated faster than the enantiomer or C2 epimers with a 2S stereochemistry, except for the D-arabinonic acid/D-ribonic acid C2 epimeric pair and the D-talonic acid/L-talonic acid enantiomeric pair (Fig. 8A and B).

For C3, C4 and C5 epimeric pairs of PHAs, the epimers with different stereochemistry between the last two carbons migrated faster than the epimers with the same stereochemistry between the last two carbons. In other words, the epimers with different stereochemistry between CX and CX-1 migrated faster than the epimers with the same stereochemistry between CX and CX-1, where X is the total number of carbons of the PHA (Fig. 8A and B).

The effective electrophoretic mobilities (μ_{eff}) of the HAs and the chiral selector (μ_{eff} vancomycin = 12.26×10^{-9} m^2 V^{-1} s^{-1}) were determined based on their respective migration times and the electroosmotic mobility of the EOF ($\mu_{EOF} = -2.94 \times 10^{-9}$. m^2 V^{-1} s^{-1}) (Table S2).

3.6. Variation of resolution, analysis time, signal intensity and limit of detection

3.6.1. Effect of vancomycin concentration

We determined the variation of chiral resolution as a function of vancomycin concentration for a representative AHA (DL-2-hydroxybutyric acid), BHA (DL-3-hydroxyoctanoic acid) and PHA (DL-gluconic acid). Increasing the concentration of vancomycin resulted in enhanced chiral separation for all HAs investigated by increasing the resolution and migration time for AHAs, BHAs, and PHAs (Fig. 9A and B). This means that a high concentration of vancomycin would always be recommended for the initial chiral analysis of an unknown HA, the vancomycin concentration may later be decreased for faster migration time, if the resolution allows it.

However, increasing the vancomycin concentration also results in a lower signal intensity and higher limit of detection (LOD; signal-to-noise ratio = 3). Fig. 9C shows that the signals corresponding to 1 mM of DL-2-

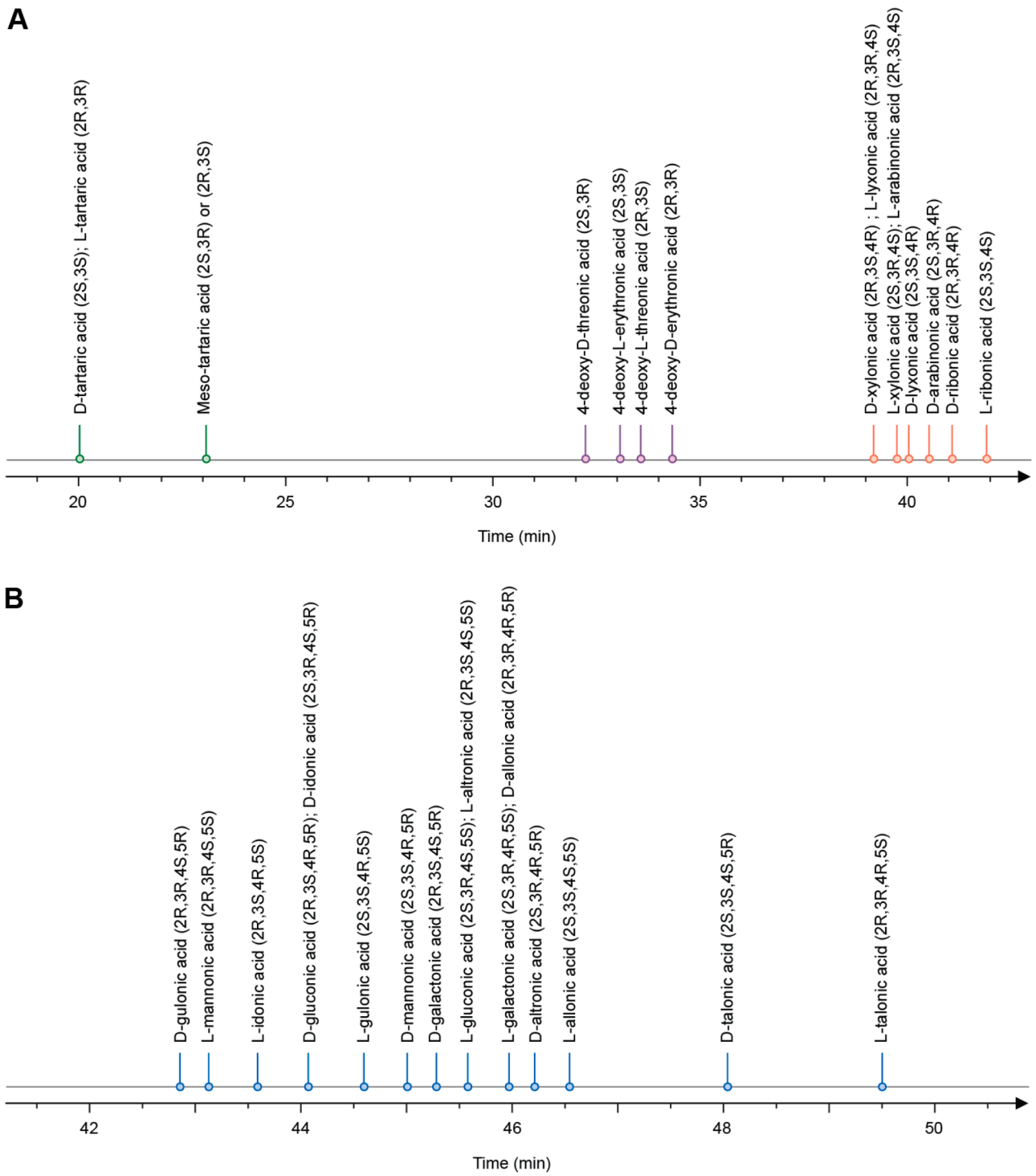

Fig. 8. Schematic representation of the chiral separation and migration times of PHAs stereoisomers. (A) Schematic representation of the chiral separations and migration times of the stereoisomers of tartaric acid (green), 2,3-dihydroxybutanoic acid (purple) and 2,3,4,5-tetrahydroxypentanoic acid (orange). (B) Schematic representation of the chiral separations and migration times of (2,3,4,5,6)-pentahydroxyhexanoic acid stereoisomers (blue). Electrophoretic conditions as in Fig. 7 for A and B .

hydroxybutyric acid, DL-3-hydroxyoctanoic acid and DL-gluconic acid decrease with an increase in vancomycin concentration. And Fig. 9D shows that the LOD of D-2-hydroxybutyric acid, D-3-hydroxybutyric acid and DL-gluconic acid increases with higher vancomycin concentrations. Therefore, if large resolution is not required, a low concentration of vancomycin is recommended.

At a fixed concentration of vancomycin, we observed that the signal of aliphatic HAs is directly proportional to their molecular weight. However, this correlation does not hold for aromatic AHAs, which are UV-absorbing, as their signal varies depending on their chromophore (Fig 10).

3.6.2. *Effect of capillary length*

We also determined the influence of capillary length on the resolution, analysis time, signal intensity and LOD for a representative AHA (DL-2-hydroxybutyric acid), BHA (DL-3-hydroxyoctanoic acid) and PHA

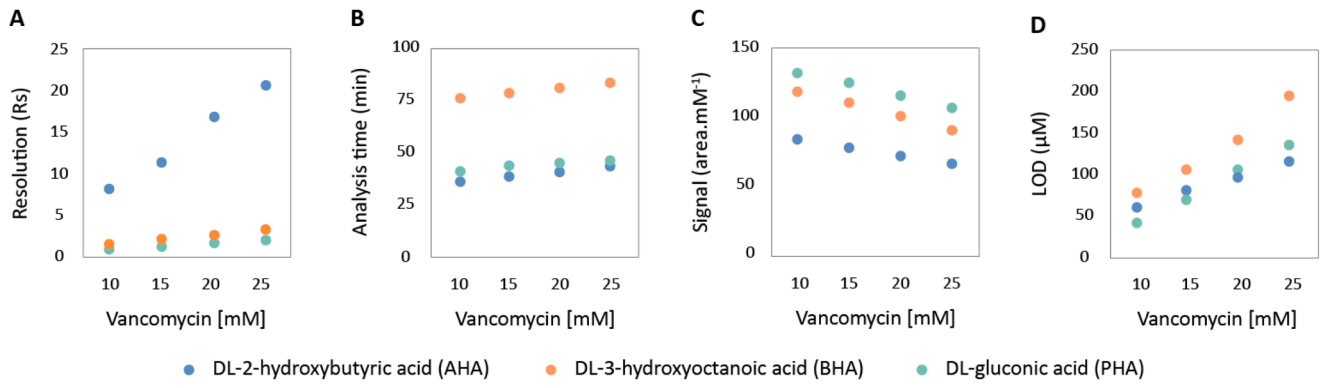

Fig. 9. Resolution, analysis time, signal intensity and limit of detection as a function of vancomycin concentration. (A) Chiral resolution as a function of vancomycin concentration. Separations were conducted with 0.5 mM of each enantiomer. (B) Analysis time as a function of vancomycin concentration. The indicated analysis time for each enantiomeric pair corresponds to the migration time of the slowest enantiomer. (C) Signal intensity as a function of vancomycin concentration. (D) LOD as a function of vancomycin concentration. The indicated LOD for each enantiomeric pair refers to the D-enantiomer. Vancomycin concentrations as indicated, other electrophoretic conditions as in Fig. 2 for A, B, C and D: .

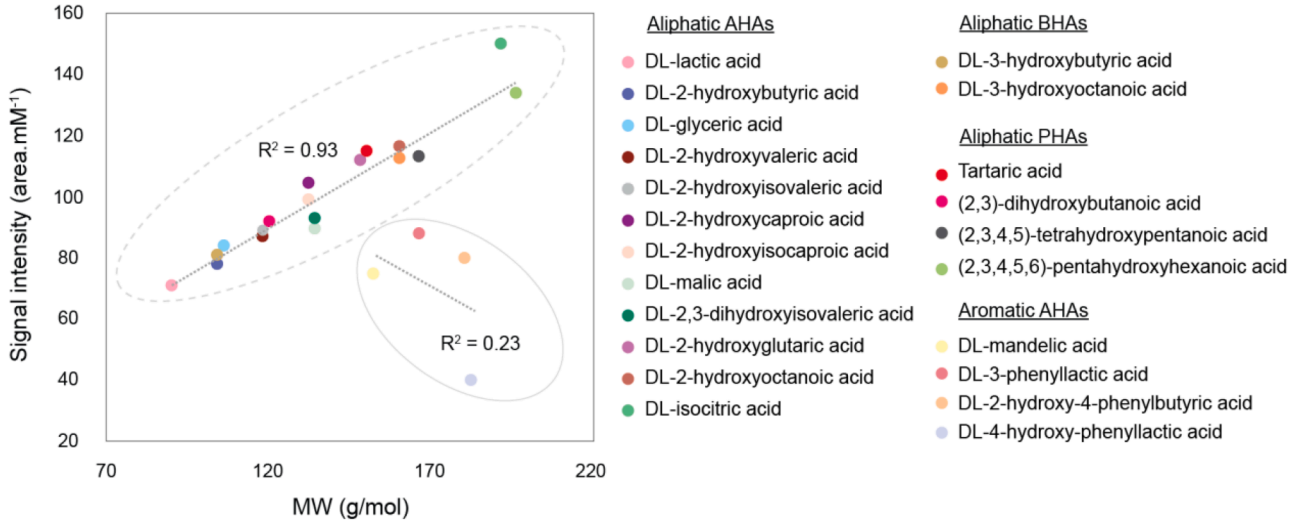

Fig. 10. Signal intensity variation as a function of HAs molecular weight. For AHAs and BHAs, we used the area corresponding to 1 mM of the enantiomeric mixture. For PHAs, we used the mean of the areas corresponding to 1 mM of each stereoisomers. Aliphatic HAs are encircled by a dashed gray line, while aromatic HAs are encircled by a solid gray line. Pearson correlation: $r(18) = 0.96$, $p < 0.001$ and $r(4) = -0.48$, $p > 0.5$. Vancomycin concentration 10 mM, other electrophoretic conditions as in Fig. 2.

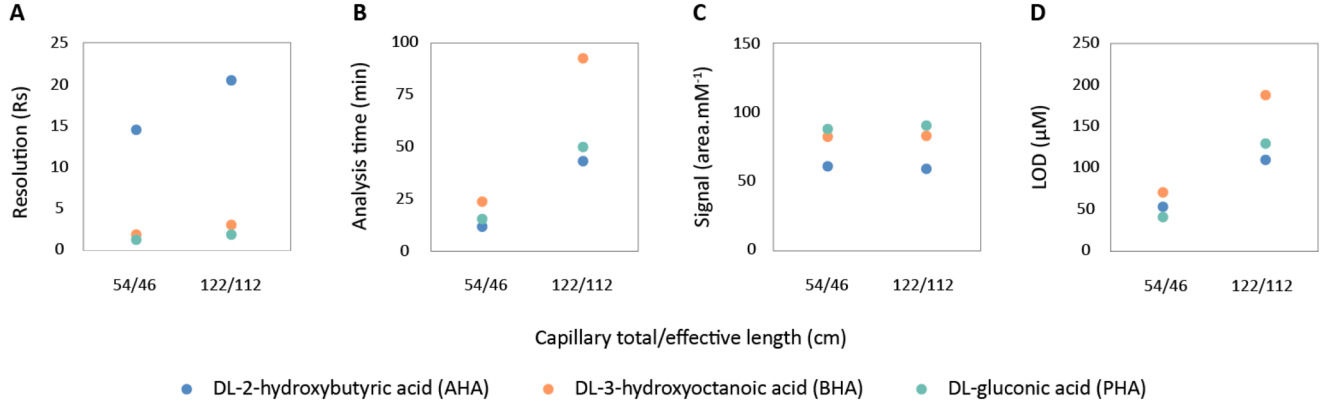

Fig. 11. Resolution, analysis time, signal intensity and LOD as a function of capillary length. (A) Chiral resolution as a function of capillary length. Separations were conducted with 0.5 mM of each enantiomer. (B) Analysis time as a function of capillary length. The indicated analysis time for each enantiomeric pair corresponds to the migration time of the slowest enantiomer. (C) Signal intensity as a function of capillary length. (D) LOD as a function of capillary length. The indicated LOD for each enantiomeric pair refers to the D-enantiomer. Electrophoretic conditions as in Fig. 2 for A, B, C, and D.

(DL-gluconic acid) (Fig. 11). We observed an enhancement of chiral resolution and a prolonged analysis time as capillary length increased (Fig. 11A and B), highlighting a trade-off between enhanced resolution and analysis time. The signal intensity remained constant but the LOD increased with the length of the capillary (Fig. 11C and D), due to the widening of the peak. Using electrophoretic conditions for optimal resolution, LOD values were in the range of 39–152 μM for aliphatic HAs and 194–447 μM for aromatic HAs (Table S2). However, it is possible to significantly reduce the LOD at the expense of resolution by lowering the vancomycin concentration as shown in Fig. 9D or by using a shorter capillary as shown in Fig. 11D. Overall, these results underscore the importance of capillary length optimization in electrophoretic separations, considering the trade-offs between resolution, analysis time, and LOD, for achieving specific analytical goals.

3.7. Analysis of complex matrices

In this section, we demonstrate the versatility of our method for analyzing complex matrices, such as in vitro enzymatic reactions and real-world samples. Utilizing GntE1, a D-gluconate C-2 epimerase from the LarA superfamily [59], we showcased the analysis of the epimerization of D-gluconate into D-mannonate over time (Fig. S1). This shows the applicability of the method in studying isomerization reactions such as racemization or epimerization of HAs, and its possible use for the determination of the stereochemical specificity and kinetic parameters of HA isomerases. Previously, we successfully applied this method to determine the kinetic parameters of tartrate epimerization by Mar2, a malate racemase and tartrate epimerase from the LarA superfamily [60]. In addition, we utilized isocitrate dehydrogenase (IDH) to monitor the decarboxylation of D-isocitrate into 2-ketoglutarate and CO_2 over time (Fig. S2). This demonstrates the efficacy of the method in studying dehydrogenation reactions involving HAs and its potential for determining the stereochemical specificity and kinetic parameters of HA dehydrogenases.

We also analyzed a zinc gluconate dietary supplement containing 353 mg of gluconate per 530 mg tablet. Employing our method, we estimated the concentration of D-gluconate, which corresponded to 95 $\pm$ 4 % of its theoretical concentration. No traces of L-gluconate were detected (Fig. S3). This validation confirms the ability of our method to identify and quantify a HA within a complex matrix.

4. Conclusions

This work presents for the first time a robust and versatile method allowing a highly efficient chiral analysis of a wide range of underivatized HAs of biological and industrial importance by CE. The significance of this method lies in its broad applicability across various fields, e.g. in pharmaceutical, biomarkers, and biochemistry research. Notably, it plays a pivotal role in the study of the LarA superfamily, a recently discovered superfamily of AHA racemases and epimerases [59,60]. Similarly, chiral analysis of BHAs is indispensable in chemical synthesis and medicinal chemistry, as BHAs serve as essential building blocks for bioactive compounds. Furthermore, the chiral analysis of underivatized PHAs, an area previously undocumented in the literature, opens new avenues for the study of aldonic sugar acids with implications across various research areas and in industry. Overall, the effectiveness of the protocol in the stereoisomeric separation of AHAs, BHAs, and PHAs underscores its suitability for the analysis of a wide range of samples containing carboxyl and hydroxyl groups. This versatility not only supports stereochemical investigations but also offers the potential to improve our understanding of complex biological and chemical systems.

In conclusion, the interest of the developed method extends to diverse applications, from exploring enzymatic mechanisms and metabolic pathways to practical uses in pharmaceutical and industrial chemistry. It offers an effective tool for chiral analysis of HAs.

CRediT authorship contribution statement

Julian Urdiain-Arraiza: Conceptualization, Data curation, Formal analysis, Funding acquisition, Investigation, Methodology, Supervision, Validation, Visualization, Writing – original draft, Writing – review & editing. **Benoît Desguin:** Funding acquisition, Project administration, Resources, Supervision, Validation, Writing – review & editing.

Declaration of Competing Interest

The authors declare that they have no known competing financial interests or personal relationships that could have appeared to influence the work reported in this paper.

Data availability

Data will be made available on request.

Acknowledgments

This research was supported by the Fonds de la Recherche Scientifique (FNRS).

Supplementary materials

Supplementary material associated with this article can be found, in the online version, at doi:10.1016/j.chroma.2023.464611.

References

[1] M.S. Van Dyk, J.L.F. Kock, A. Botha, Hydroxy long-chain fatty acids in fungi, World J. Microbiol. Biotechnol. 10 (1994) 495–504, https://doi.org/10.1007/BF00367653.
[2] A. Kornhauser, S.G. Coelho, V.J. Hearing, Applications of hydroxy acids: classification, mechanisms, and photoactivity, Clin. Cosmet. Investig. Dermatol. 3 (2010) 135–142, https://doi.org/10.2147/ccid.s9042.
[3] B.A. Green, R.J. Yu, E.J. Van Scott, Clinical and cosmeceutical uses of hydroxyacids, Clin. Dermatol. 27 (2009) 495–501, https://doi.org/10.1016/j.clindermatol.2009.06.023.
[4] P. Babilas, U. Knie, C. Abels, Cosmetic and dermatologic use of alpha hydroxy acids, J. Ger. Soc. Dermatol. 10 (2012) 488–491, https://doi.org/10.1111/j.1610-0387.2012.07939.x.
[5] G.M. Coppola, H.F. Schuster, Alpha-Hydroxy Acids in Enantioselective Syntheses, Wiley-VCH, Weinheim, 1997.
[6] E. Gracia-Moreno, R. Lopez, V. Ferreira, Quantitative determination of five hydroxy acids, precursors of relevant wine aroma compounds in wine and other alcoholic beverages, Anal. Bioanal. Chem. 407 (2015) 7925–7934, https://doi.org/10.1007/s00216-015-8959-9.
[7] G. Zhao, G. Kuang, J. Li, H. Hadiatullah, Z. Chen, X. Wang, Y. Yao, Z.H. Pan, Y. Wang, Characterization of aldehydes and hydroxy acids as the main contribution to the traditional Chinese rose vinegar by flavor and taste analyses, Food Res. Int. (2020) 129, https://doi.org/10.1016/j.foodres.2019.108879.
[8] A. Basu, K.R. Kunduru, J. Katzhendler, A.J. Domb, Poly(α-hydroxy acid)s and poly (α-hydroxy acid-co-α-amino acid)s derived from amino acid, Adv. Drug Deliv. Rev. 107 (2016) 82–96, https://doi.org/10.1016/j.addr.2016.08.003.
[9] T. Chand Bhalla, V. Kumar, S. Kant Bhatia, T.C. Bhalla, S.K. Bhatia, Hydroxy acids: production and applications, Adv. Ind. Biotechnol. (2014) 56–76. https://www.researchgate.net/publication/311494113.
[10] J. McConathy, M.J. Owens, Stereochemistry in drug action, J. Clin. Psychiatry 5 (2003), https://doi.org/10.4088/pcc.v05n0202.
[11] D. Matelska, I.G. Shabalin, J. Jabłońska, M.J. Domagalski, J. Kutner, K. Ginalski, W. Minor, Classification, substrate specificity and structural features of D-2-hydroxyacid dehydrogenases: 2HADH knowledgebase, BMC Evol. Biol. 18 (2018) 1–23, https://doi.org/10.1186/s12862-018-1309-8.
[12] N. Daniel, R.T. Nachbar, T.T.T. Tran, A. Ouellette, T.V. Varin, A. Cotillard, L. Quinquis, A. Gagné, P. St-Pierre, J. Trottier, B. Marcotte, M. Poirel, M. Saccareau, M.J. Dubois, P. Joubert, O. Barbier, H. Koutnikova, A. Marette, Gut microbiota and fermentation-derived branched chain hydroxy acids mediate health benefits of yogurt consumption in obese mice, Nat. Commun. (2022) 13, https://doi.org/10.1038/s41467-022-29005-0.
[13] C. Calderón, M. Lämmerhofer, Chiral separation of short chain aliphatic hydroxycarboxylic acids on cinchonan carbamate-based weak chiral anion exchangers and zwitterionic chiral ion exchangers, J. Chromatogr. A. 1487 (2017) 194–200, https://doi.org/10.1016/j.chroma.2017.01.060.

[14] L.-G. Bogos, I.-E. Pralea, R.-C. Moldovan, C.A. Iuga, Indirect enantioseparations: recent advances in chiral metabolomics for biomedical research, Int. J. Mol. Sci. (2022) 23, https://doi.org/10.3390/ijms23137428.
[15] A. Van Eeckhaut, Y. Michotte, Chiral separations by capillary electrophoresis: recent developments and applications, Electrophoresis 27 (2006) 2880–2895, https://doi.org/10.1002/elps.200500375.
[16] S. Kodama, A. Yamamoto, A. Matsunaga, Direct chiral resolution of aliphatic α-hydroxy acids using 2-hydroxypropyl-β-cyclodextrin in capillary electrophoresis, Analyst 124 (1999) 55–59, https://doi.org/10.1039/a807351a.
[17] L. Saavedra, C. Barbas, Optimization of the separation lactic acid enantiomers in body fluids by capillary electrophoresis, J. Chromatogr. B. 766 (2002) 235–242, https://doi.org/10.1016/S0378-4347(01)00473-X.
[18] S. Okubo, F. Mashige, M. Omori, Y. Hashimoto, K. Nakahara, H. Kanazawa, Y. Matsushima, Enantiomeric determination of L- and D-lactic acid in human cerebrospinal fluid by chiral ligand exchange high-performance liquid chromatography, Biomed. Chromatogr. 14 (2000) 474–477, https://doi.org/10.1002/1099-0801(200011)14:7<474::AID-BMC995>3.0.CO;2-3.
[19] C. Calderón, J. Horak, M. Lämmerhofer, Chiral separation of 2-hydroxyglutaric acid on cinchonan carbamate based weak chiral anion exchangers by high-performance liquid chromatography, J. Chromatogr. A. 1467 (2016) 239–245, https://doi.org/10.1016/j.chroma.2016.05.042.
[20] E.J. Franco, H. Hofstetter, O. Hofstetter, Determination of lactic acid enantiomers in human urine by high-performance immunoaffinity LC-MS, J. Pharm. Biomed. Anal. 49 (2009) 1088–1091, https://doi.org/10.1016/j.jpba.2009.01.033.
[21] M.S. Rashed, M. Alamoudi, H.Y. Aboul-Enein, Chiral liquid chromatography tandem mass spectrometry in the determination of the configuration of 2-hydroxyglutaric acid in urine, Biomed. Chromatogr. 14 (2000) 317–320, https://doi.org/10.1002/1099-0801(200008)14:5<317::AID-BMC989>3.0.CO;2-V.
[22] S. Kodama, A. Taga, A. Yamamoto, Y. Ito, Y. Honda, K. Suzuki, T. Yamashita, T. Kemmei, S.I. Aizawa, Enantioseparation of DL-isocitric acid by a chiral ligand exchange CE with Ni(II)-D-quinic acid system, Electrophoresis 31 (2010) 3586–3591, https://doi.org/10.1002/elps.201000320.
[23] C. Desiderio, Z. Aturki, S. Fanali, Separation of α-hydroxy acid enantiomers by high performance capillary electrophoresis using copper(II)-L-amino acid and copper (II)-aspartame complexes as chiral selectors in the background electrolyte, Electrophoresis 15 (1994) 864–869, https://doi.org/10.1002/elps.11501501122.
[24] A. Nardi, A. Eliseev, P. Bocek, S. Fanali, Use of charged and neutral cyclodextrins in capillary zone electrophoresis : enantiomeric resolution of some 2-hydroxy acids, J. Chromatogr. 638 (1993) 247–253, https://doi.org/10.1016/0021-9673(93)83435-U.
[25] M.G. Schmid, O. Lecnik, U. Sitte, G. Gubitz, Application of ligand-exchange capillary electrophorersis to the chiral separation of α-hydroxy acids and β-blockers, J. Chromatogr. A. 875 (2000) 307–314, https://doi.org/10.1016/S0021-9673(99)01333-3.
[26] E. Pittler, N. Grawatsch, D. Paul, G. Gübitz, M.G. Schmid, Enantioseparation of amino acids, α-hydroxy acids, and dipeptides by ligand-exchange CEC using silica-based chiral stationary phases, Electrophoresis 30 (2009) 2897–2904, https://doi.org/10.1002/elps.200900092.
[27] S. Tong, M. Shen, D. Cheng, Y. Zhang, Y. Ito, J. Yan, Chiral ligand exchange high-speed countercurrent chromatography: mechanism and application in enantioseparation of aromatic α-hydroxyl acids, J. Chromatogr. A. 1360 (2014) 110–118, https://doi.org/10.1016/j.chroma.2014.07.057.
[28] I. Varfaj, M. Protti, A. Di Michele, A. Macchioni, W. Lindner, A. Carotti, R. Sardella, L. Mercolini, Efficient enantioresolution of aromatic α-hydroxy acids with Cinchona alkaloid-based zwitterionic stationary phases and volatile polar-ionic eluents, Anal. Chim. Acta. (2021) 1180, https://doi.org/10.1016/j.aca.2021.338928.
[29] S. Tong, H. Zhang, M. Shen, Y. Ito, J. Yan, Enantioseparation of mandelic acid derivatives by high performance liquid chromatography with substituted β-cyclodextrin as chiral mobile phase additive and evaluation of inclusion complex formation, J. Chromatogr. B. 962 (2014) 44–51, https://doi.org/10.1016/j.jchromb.2014.05.026.
[30] F. Ianni, Z. Pataj, H. Gross, R. Sardella, B. Natalini, W. Lindner, M. Lämmerhofer, Direct enantioseparation of underivatized aliphatic 3-hydroxyalkanoic acids with a quinine-based zwitterionic chiral stationary phase, J. Chromatogr. A. 1363 (2014) 101–108, https://doi.org/10.1016/j.chroma.2014.03.060.
[31] R. Karongo, J. Jiao, H. Gross, M. Lämmerhofer, Direct enantioselective gradient reversed-phase ultra-high performance liquid chromatography tandem mass spectrometry method for 3-hydroxy alkanoic acids in lipopeptides on an immobilized 1.6μm amylose-based chiral stationary phase, J. Sep. Sci. 44 (2021) 1875–1883, https://doi.org/10.1002/jssc.202100104.
[32] X. Fu, Z. Xu, M. Gawaz, M. Lämmerhofer, UHPLC-MS/MS method for chiral separation of 3-hydroxy fatty acids on amylose-based chiral stationary phase and its application for the enantioselective analysis in plasma and platelets, J. Pharm. Biomed. Anal. (2023) 223, https://doi.org/10.1016/j.jpba.2022.115151.
[33] S. Kodama, A. Yamamoto, A. Matsunaga, K. Hayakawa, Direct chiral resolution of tartaric acid in food products by ligand exchange capillary electrophoresis using copper(II)-D-quinic acid as a chiral selector, J. Chromatogr. A. 932 (2001) 139–143, https://doi.org/10.1016/S0021-9673(01)01228-6.
[34] R. Knob, J. Petr, J. Ševčík, V. Maier, Enantioseparation of tartaric acid by ligand-exchange capillary electrophoresis using contactless conductivity detection, J. Sep. Sci. 36 (2013) 3426–3431, https://doi.org/10.1002/jssc.201300507.
[35] G. Hancu, L.A. Papp, B. Szekely-Szentmiklosi, H. Kelemen, The use of antibiotics as chiral selectors in capillary electrophoresis: a review, Molecules (2022) 27, https://doi.org/10.3390/molecules27113601.
[36] S. Fanali, B. Chankvetadze, Some thoughts about enantioseparations in capillary electrophoresis, Electrophoresis 0 (2019) 2420–2437, https://doi.org/10.1002/elps.201900144.
[37] A. Ewing, R. Wallingford, T. Olefirowicz, Capillary electrophoresis, Anal. Chem. 61 (1989) 292A–303A, https://doi.org/10.1021/ac00179a002.
[38] W. Schtitzner, G. Caponecchi, S. Fanali, A. Rizzi, E. Kenndler, Improved separation of diastereomeric derivatives of enantiomers by a physical network of linear polyvinylpyrrolidone applied as pseudophase in capillary zone electrophoresis, Electrophoresis 15 (1994) 769–773, https://doi.org/10.1002/elps.11501501107.
[39] F. Kilár, S. Hjertén, Fast and high resolution analysis of human serum transferrin by high performance isoelectric focusing in capillaries, Electrophoresis 10 (1989) 23–29, https://doi.org/10.1002/elps.1150100107.
[40] W. Wang, F. Zhou, L. Zhao, J.R. Zhang, J.J. Zhu, Measurement of electroosmotic flow in capillary and microchip electrophoresis, J. Chromatogr. A. 1170 (2007) 1–8, https://doi.org/10.1016/j.chroma.2007.08.083.
[41] C. Desiderio, S. Fanali, Chiral analysis by capillary electrophoresis using antibiotics as chiral selector, J. Chromatogr. A. 807 (1998) 37–56, https://doi.org/10.1016/S0021-9673(98)00061-2.
[42] H.Y. Aboul-Enein, I. Ali, Macrocyclic antibiotics as effective chiral selectors for enantiomeric resolution by liquid chromatography and capillary electrophoresis, Chromatographia 52 (2000) 679–691, https://doi.org/10.1007/BF02490991.
[43] T.J. Ward, A.B. Farris, Chiral separations using the macrocyclic antibiotics: a review, J. Chromatogr. A. 906 (2001) 73–89, https://doi.org/10.1016/S0021-9673(00)00941-9.
[44] T.J. Ward, C. Dann, A.P. Brown, Separation of enantiomers using vancomycin in a countercurrent process by suppression of electroosmosis, Chirality 8 (1996) 77–83, https://doi.org/10.1002/(SICI)1520-636X(1996)8:1<77::AID-CHIR13>3.0.CO;2-P.
[45] A. Amini, U. Paulsen-Sörman, D. Westerlund, Principle and applications of the partial filling technique in capillary electrophoresis, Chromatographia 50 (1999) 497–506, https://doi.org/10.1007/BF02490748.
[46] A. Amini, Recent developments in chiral capillary electrophoresis and applications of this technique to pharmaceutical and biomedical analysis, Electrophoresis 22 (2001) 3107–3130, https://doi.org/10.1002/1522-2683(200109)22:15<3107::AID-ELPS3107>3.0.CO;2-Z.
[47] L. Valtcheva, J. Mohammad, G. Pettersson, S. Hjertén, Chiral separation of β-blockers by high-performance capillary electrophoresis based on non-immobilized cellulase as enantioselective protein, J. Chromatogr. 638 (1993) 263–267, https://doi.org/10.1016/0021-9673(93)83437-W.
[48] P. Bednar, Z. Aturki, Z. Stransky, S. Fanali, Chiral analysis of UV nonabsorbing compounds by capillary electrophoresis using macrocyclic antibiotics: 1. Separation of aspartic and glutamic acid enantiomers, Electrophoresis 22 (2001) 2129–2135, https://doi.org/10.1002/1522-2683(20017)22:11<2129::AID-ELPS2129>3.0.CO;2-J.
[49] L. Tan, Y. Wang, X. Liu, H. Ju, J. Li, Simultaneous determination of L- and D-lactic acid in plasma by capillary electrophoresis, J. Chromatogr. B. 814 (2005) 393–398, https://doi.org/10.1016/j.jchromb.2004.10.059.
[50] W. Pormsila, X.Y. Gong, P.C. Hauser, Determination of the enantiomers of α-hydroxy- and α-amino acids in capillary electrophoresis with contactless conductivity detection, Electrophoresis 31 (2010) 2044–2048, https://doi.org/10.1002/elps.201000127.
[51] V. Maier, J. Petr, R. Knob, J. Horáková, J. Ševčík, Electrokinetic partial filling technique as a powerful tool for enantiomeric separation of DL-lactic acid by CE with contactless conductivity detection, Electrophoresis 28 (2007) 1815–1822, https://doi.org/10.1002/elps.200600578.
[52] S. Kodama, A. Yamamoto, A. Matsunaga, T. Soga, K. Minoura, Direct chiral resolution of lactic acid in food products by capillary electrophoresis, J. Chromatogr. A. 875 (2000) 371–377, https://doi.org/10.1016/S0021-9673(99)01005-5.
[53] Q. Ren, K. Ruth, L. Thöny-Meyer, M. Zinn, Enantiomerically pure hydroxycarboxylic acids: current approaches and future perspectives, Appl. Microbiol. Biotechnol. 87 (2010) 41–52, https://doi.org/10.1007/s00253-010-2530-6.
[54] J. Sjögren, J. Magnusson, A. Broberg, J. Schnürer, L. Kenne, Antifungal 3-hydroxy fatty acids from Lactobacillus plantarum MiLAB 14, Appl. Environ. Microbiol. 69 (2003) 7554–7557, https://doi.org/10.1128/AEM.69.12.7554-7557.2003.
[55] J. Mierziak, M. Burgberger, W. Wojtasik, 3-Hydroxybutyrate as a metabolite and a signal molecule regulating processes of living organisms, Biomolecules 11 (2021) 1–21, https://doi.org/10.3390/biom11030402.
[56] N.H. Youssef, K.E. Duncan, M.J. McInerney, Importance of 3-hydroxy fatty acid composition of lipopeptides for biosurfactant activity, Appl. Environ. Microbiol. 71 (2005) 7690–7695, https://doi.org/10.1128/AEM.71.12.7690-7695.2005.
[57] M. Hilvo, I. De Santiago, P. Gopalacharyulu, W.D. Schmitt, J. Budczies, M. Kuhberg, M. Dietel, T. Aittokallio, F. Markowetz, C. Denkert, J. Sehouli, C. Frezza, S. Darb-Esfahani, E.I. Braicu, Accumulated metabolites of hydroxybutyric acid serve as diagnostic and prognostic biomarkers of ovarian high-grade serous carcinomas, Cancer Res. 76 (2016) 796–804, https://doi.org/10.1158/0008-5472.CAN-15-2298.
[58] T. Mehtiö, M. Toivari, M.G. Wiebe, A. Harlin, M. Penttilä, A. Koivula, Production and applications of carbohydrate-derived sugar acids as generic biobased

chemicals, Crit. Rev. Biotechnol. 36 (2016) 904–916, https://doi.org/10.3109/07388551.2015.1060189.
[59] B. Desguin, J. Urdiain-Arraiza, M. Da Costa, M. Fellner, J. Hu, R.P. Hausinger, T. Desmet, P. Hols, P. Soumillion, Uncovering a superfamily of nickel-dependent hydroxyacid racemases and epimerases, Sci. Rep. (2020) 10, https://doi.org/10.1038/s41598-020-74802-6.
[60] S. Gatreddi, J. Urdiain-Arraiza, B. Desguin, R.P. Hausinger, J. Hu, Structural and mutational characterization of a malate racemase from the LarA superfamily, BioMetals (2022), https://doi.org/10.1007/s10534-022-00372-x.